Fast Decomposed Energy Flow in Large-Scale Integrated Electricity-Gas-Heat Energy Systems

Hamid Reza Massrur, *Student Member, IEEE*, Taher Niknam, *Member, IEEE*, Jamshid Aghaei, *Senior Member, IEEE*, Miadreza Shafie-khah, *Senior Member, IEEE*, and João P. S. Catalão, *Senior Member, IEEE*

Abstract—In this paper, a new decomposing strategy is proposed to solve the power flow problem in the large-scale Multi-Energy Carrier (MEC) systems, including gas, electrical and heating sub-networks. This strategy has been equipped with a novel non-iterative method named Holomorphic Embedding (HE) to solve the energy flow of the electrical sub-network. Moreover, it benefits from the less-computational graph method for solving the energy flows of the heating sub-network. The HE method unlike initial-guess iterative methods guarantees to find power flow solution if there is a solution. In addition, it finds only the operational power flow solution without concern about the convergence of the solution. In the proposed strategy, the decomposing method decouples various energy flows of sub-networks without losing the major benefits of the simultaneous analysis of the sub-networks and losing accuracy. Moreover, the proposed decomposing strategy has more reliability and faster than the Newton-Raphson technique. In order to demonstrate the efficiency and superiority of the proposed decomposing strategy on solving the large-scale MEC systems, the strategy is tested on three large-scale multi-energy carrier case studies.

***Index Terms*—Multi-Energy Carrier, Energy Hub, Heating Network, Decomposed Energy Flow, Holomorphic Embedding, Graph Theory.**

Nomenclature

a) Electrical Network Variables and Parameters

d_V	The percentage voltage magnitude deviation of DNR-PFMEC and DHG-PFMEC methods from the results of NR-PFMEC method (%).
d_ θ	The percentage voltage angle deviation of DNR-PFMEC and DHG-PFMEC methods from the results of NR-PFMEC method (%).
L_e	Electrical load *(MW)*
N_E	Number of electrical buses
P_e	Electrical power received by electrical network *(MW)*
P_i^{CHP} , Q_i^{CHP}	Electric active and reactive power of CHPs in ith bus *(MVA)*
P_i^{dem}, Q_i^{dem}	Electric active and reactive power demand in ith Bus *(MVA)*
P_i^{gen}, Q_i^{gen}	Electric active and reactive power of generators in ith bus *(MVA)*
P_i^{Pump}	Electric power consumption by heating pumps *(MW)*
P_i^{Comp}	Electric power consumption by gas compressors *(MW)*
P_i	The power generation at bus i *(P.U.)*
Q_i^{SH}	Injected reactive power by shunt capacitors *(MVAR)*
S	Complex power
V_i	Voltage magnitude at bus ith *(P.U.)*
V_i^{sp}	The voltage magnitude at bus i *(P.U.)*
Y_{ij}	Admittance of the transmission line between nodes i to j *(P.U.)*
$Y_{ik\ ,series}$	Related to the branch series in the line data
$Y_{i\ shunt}$	Related to the shunt element in the line data
θ_i	Voltage angle at bus ith

b) Natural Gas Network Variables and Parameters

C_{gk}	Pipeline constant between nodes gth and kth ($\sqrt{K.mm}$).
d_π	The percentage pressure deviation of DNR-PFMEC and DHG-PFMEC methods from the results of NR-PFMEC method (%).
D_{gk}^{GL}	Diameter of pipeline between nodes g to k *(mm)*
E_p	Absolute rugosity of natural gas pipeline *(mm)*
f_g^{Source}	Injected gas flow at node gth *(m^3/day)*
f_g^{dem}	Gas demand at node gth *(m^3/day)*
f_{gk}	Gas flow through the pipeline connected between nodes gth and kth *(m^3/day)*
f_G^{boilre}	Gas consumed by boilers *(m^3/day)*

Manuscript received June 11, 2017; revised October 1, 2017 and December 13, 2017; accepted January 17, 2018. Date of publication January 23, 2018; date of current version September 18, 2018. The work of J. P. S. Catal˜ao was supported in part by the FEDER funds through COMPETE 2020, in part by the Portuguese funds through FCT, under Projects SAICT-PAC/0004/2015—POCI-01-0145-FEDER-016434, POCI- 01-0145-FEDER-006961, UID/EEA/50014/2013, UID/CEC/50021/2013, and UID/EMS/00151/2013, and in part by the EU 7th Framework Programme FP7/2007-2013 under Grant Agreement 309048. Paper no. TSTE-00539-2017. *(Corresponding author: Jo˜ao P. S. Catal˜ao.)*

H. R. Massrur and T. Niknam are with the Department of Electrical and Electronics Engineering, Shiraz University of Technology, Shiraz 13876-71557, Iran (e-mail: h.massrur@sutech.ac.ir; niknam@sutech.ac.ir).

J. Aghaei is with the Department of Electrical and Electronics Engineering, Shiraz University of Technology, Shiraz 13876-71557, Iran, and also with the Department of Electric Power Engineering, Norwegian University of Science and Technology (NTNU), Trondheim NO-7491, Norway (e-mail: aghaei@sutech.ac.ir).

M. Shafie-khah is with the Centre for Mechanical and Aerospace Science and Technologies, University of Beira Interior, Covilh˜a 6201-001, Portugal (e-mail: miadreza@ubi.pt).

J. P. S. Catal˜ao is with the Institute for Systems and Computer Engineering, Technology and Science, Faculty of Engineering, University of Porto, Porto 4200-465, Portugal, with the Centre for Mechanical and Aerospace Science and Technologies,University of Beira Interior, Covilh˜a 6201-001, Portugal, and also with the INESC-ID, Instituto Superior T´ecnico, University of Lisbon, Lisbon 1049-001, Portugal (e-mail: catalao@ubi.pt).

f_{gk}^{comp} Gas consumed by gas turbo compressors *(m^3/day)*
f_G^{chp} Gas consumed by CHP units *(m^3/day)*
f^{GG} Gas consumed by gas-fired generators *(m^3/day)*
GHV Gross heating value *(MBTU/m^3)*
H_p^{gk} Slope pipeline correction for the pipeline *(kPa^2)*
L_{gk} Length of the pipeline between nodes g to k *(km)*
π_g , π_k Gas pressure at nodes gth and kth *(kPa)*
π_a^{gk} Average pressure for the pipeline *(kPa)*
T_0 Base temperature *(K)*
T_G Gas temperature at the entry of the compressor *(K)*
π_0 Base pressure *(kPa)*
P_g Gas power received by Gas network *(MSCM/h)*
χ_{gk}^{GL} Friction factor of the gas pipeline between nodes g to k *(Dimensionless)*
η_t^{chp} Efficiency of CHP
T_a Average gas flowing temperature *(K)*
Z_a Gas compressibility factor at flowing temperature *(Dimensionless)*
λ_G Specific heat ratio of natural gas *(Dimensionless)*
η_{gk}^{comp} Compressor efficiency *(Dimensionless)*
γ_G Gas gravity *(Dimensionless)*
α_{gk}^{comp}, β_{gk}^{comp}, γ_{gk}^{comp} Consumption coefficients of the compressors *(Dimensionless)*

c) Heating Network Variables and Parameters

$(a_{k,j})$ The elements of incidence matrix (A)
a^{boil}, b^{boil} Coefficients that depend on the part-load performance of the boiler.
d_T The percentage temperature deviation of DNR-PFMEC and DHG-PFMEC methods from the results of NR-PFMEC method (%).
L Pipeline length *(Km)*
L_h Heating load *(MW)*
g The gravity $(Kg.m/S^2)$
H_P Pump head *(m)*
η^{HP} Pump efficiency (*Dimensionless)*
Φ_h^{boiler} Injected heat power by CHP at node hth *(MW)*
Φ_h^{CHP} Injected heat power by CHP at node hth *(MW)*
Φ_h^{dem} Heat power demand at node hth *(MW*
$\Phi_H^{boil,max}$ Maximum heat power produced by boiler (*MW*)
$\dot{m}$ The mass flow rate in the pipes *(kg/s)*
$\dot{m}_q$ Injected or discharged mass flow rate from sources and loads *(kg/s)*
$\dot{m}_{hb}$ Mass flow rate through the pipeline between nodes hth to bth *(kg/s)*
$\dot{m}_H^{HP}$ Mass flow of water through heat pump
c_p Specific heat capacity of water *(KJ/KgK)*
P_h Heating power received by heating network *(MW)*
T_{start}, h Supply temperature at nod hth *(C^o)*
T_{end}, h Return temperature at node hth *(C^o)*
U Heat transition coefficient *(W/mK)*
T_g Ground temperature *(C^o)*
ρ_W Water density (Kg/m^3)

d) Acronyms

HE Holomorphic Embedding
CHP Combined Heat and Power
MEC Multi-Energy Carrier
PF Power Flow
PFMEC Power Flow of Multi-Energy Carrier
NR Newton-Raphson
DHG-PFMEC Decomposed power flow of multi-energy carrier strategy with holomorphic and graph methods
NR-PFMEC Newton-Raphson technique for power flow of multi-energy carrier
DNR-PFMEC Decomposed Newton-Raphson technique for power flow of multi-energy carrier

I. Introduction

NOWADAYS, reliable and economic effects of supplying energy cause that many interdependencies have been created among various forms of energy carriers. Among energy carriers, electrical, natural gas and heating sub-networks have more interdependencies [1], [2]. For example, in some areas various cooling and heating loads must be supplied by electrical energy. Moreover, many generators in the power system are gas-fired generators. Growing new interdependent equipment such as Combined Heat and Power (CHP), gas-fired boilers and etc. have increased interdependencies among energy carriers.

The energy carrier networks are commonly modeled as a separate subsystem. Many previous works in the literature have been presented to individually schedule these sub-systems [3]-[5]. However, significantly increasing in the utilization of the equipment that creates interdependencies among various energy infrastructures blemishes the reliable operation of sub-networks. However, it can create economic opportunities for enhancing the supply efficiency of energy systems. Recently, an integrated view of energy carrier networks has been proposed named Multi-Energy Carrier (MEC) systems in which energy carrier networks are simultaneously operated. In this regard, the energy hub concept has been developed in order to analysis the integrated MEC systems. The initial idea about the energy hub has been suggested in [6]–[7]. An energy hub can be defined as an interface among the power generation units, the energy consumers and transmission infrastructures [7]. The energy hub has a number of advantages including diversity in the energy supplying, possibility of energy storage and increasing the reliability of MEC systems [8].

In the secure operation of a MEC system, the Power Flow (PF) problem plays a remarkable role in the MEC system analysis. Moreover, the PF of Multi-Energy Carrier (PFMEC) system lays the basis for optimal operation and reliable planning analysis of these systems. The interdependencies among MEC networks affect the energy flow of the mentioned

systems. The few recent studies in the field of MEC systems try to focus on the impact of interdependent operations of MEC networks, e.g., electricity and natural gas networks [9]–[10]. In [11], gas and electrical infrastructures have taken into account as networks composed of nodes and arcs. However, in this study the technical operating parameters of the infrastructures are omitted in the model. A method to evaluate the gas network based on the Newton-Raphson method is suggested in [12] but the effects of the heating network on electrical and gas sub-networks are neglected. In [13], the conceptual framework for energy flow in an MEC system has been investigated utilizing a 3-bus system. However, the proposed framework has this drawback that is difficult to solve the PFMEC problem regarding nonlinear and non-convex characteristics of the large-scale energy hubs. The coupling of the gas and the electrical infrastructures is clearly investigated in [14] through an energy hub. In this study, the energy hub represents the energy interactions via coupling matrices whose elements correspond to efficiency and conversion factors of hub components. However, this energy hub model is established only for the equal input and output numbers and constant component efficiencies which do not have generality for all hub models. A comprehensive framework in [15] has been proposed to analyze distributed multi-generation systems for the purpose of identifying their potential to participate in real-time demand response programs. Moreover, in [16] a model for external dependencies within a multi-generation energy hub has been presented. This model is used to introduce carrier-based demand response programming. The interaction impacts of the heating and the electrical networks are evaluated in [17] but the significant interaction impacts of the gas network on these networks are not involved. In [18], a bilateral optimization is proposed to solve the optimal power flow of a MEC system. In this study, dispatch factors and slack variables have been used to decompose the optimal PF of a MEC system into separate optimal PF for each sub-network. The utilized dispatch factors and slack variables cannot consider the non-constant efficiency of the hub equipment. Moreover, the study cannot address the flow value of important equipment like electrical compressors, electrical pumps and gas-fired generators. In [19], the energy flows of the electrical, gas and heating networks are studied based on Newton-Raphson method. However, the proposed model is not capable into the fast power flow analysis of a real large-scale MEC due to the inversing calculation of a big variable Jacobian matrix for three sub-networks in the each iteration of Newton-Raphson method. Another disadvantage of this method is that Jacobian matrix components must be calculated in the each iteration. Increasing in the system scale increases the matrix size. The above previous energy flow methods for a MEC system can be classified into two main categories: 1-Using decomposing technique for only one hub with pre- determined dispatch factors 2- Utilizing Newton-Raphson technique with a big Jacobian matrix for all networks of system.

In the first category pre-determined dispatch factors are utilized in order to how much of the gas transmit to a CHP and how much transmit to a boiler in the hub. These techniques need to determine dispatch factors before energy flow analysis. Moreover, in these techniques the number of input energy carriers and output energy carriers should be equal. These techniques express the relations between input and output of an energy hub by a linear matrix including dispatch factors and constant linear efficiencies like Refs [10], [13], [15], [16] and [18]. However, with non-linear efficiency of hub equipment, these techniques face to a critical challenge and are not a realistic operational method. For surmounting the difficulties and issues related to methods in the category 1, the Newton-Raphson technique with a simultaneous Jacobian matrix for all networks of the MEC system is presented in Ref. [19]. As has been subsequently shown the Newton technique may be unsuitable for a large MEC system and cannot be converged. This is due to Newton-Raphson method creates a big Jacobian matrix with various large and low values for three networks which these various large and low values conduct the Newton method not to be converged.

To the best of authors' knowledge, none of the previous publications that investigate the PFMEC systems including electrical, gas and heating sub-networks have successfully suggested a fast and reliable method which be applicable to large-scale systems without sub-network simplification.

In order to solve the large-scale PFMEC problem with the reliable method, this paper proposes a new decomposing strategy. In this context, decomposing method decouples various energy flows of sub-networks without losing the major benefits of the simultaneous analysis of sub-networks and losing accuracy. The proposed decomposing energy flow procedure has two advantages: 1-Causes that the solving of the multi-energy carrier flow problem is faster than Newton-Raphson technic with a big Jacobian matrix for the whole of multi-carrier system. 2- In the decomposed PFMEC analysis, we can use different methods for each sub-network that they can quickly solve the PF problem of sub-networks instead of Newton technique for all sub-networks. Accordingly, this paper employs the novel Holomorphic Embedding (HE) method for solving the electrical power flow and less-computational graph theory method for solving the heat power flow. The HE is a novel non-iterative approach to solve the electrical power flow problems [20].

TABLE I: TAXONOMY OF THE PROPOSED DECOMPOSED ENERGY FLOW STRATEGY EQUIPPED WITH HE AND GRAPH METHODS AND THE PREVIOUS LITERATURE

Reference	Year	Sub-Network Considering			Non-constant efficiency	Decomposed method	Interdependent equipment with details	Large-scale capability	Solution Quality	
		Electrical (Ac power flow)	Gas sub-network	Heat sub-network					Reliable Solution	Speed
[2]	2016	No	No	Yes	No	Yes	Yes	Yes	Yes	++
[9]	2016	Yes	Yes	No	No	Yes	No	Yes	No	+
[10]	2016	Yes	Yes	No	No	Yes	No	Yes	No	+
[12]	2012	Yes	Yes	No	No	No	Yes	No	No	+
[13]	2007	Yes	Yes	No	No	Yes	No	No	No	+
[15]	2013	Yes	Yes	No	Yes	Yes	No	Yes	No	+

[16]	2015	Yes	Yes	No	No	Yes	No	Yes	No	+
[17]	2016	Yes	No	Yes	No	No	Yes	Yes	No	++
[18]	2014	Yes	Yes	No	No	Yes	No	Yes	No	+
[19]	2016	Yes	Yes	Yes	Yes	No	Yes	No	No	+
This Paper	-	Yes	Yes	Yes	Yes	Yes	Yes	Yes	Yes	+++

Unlike iterative methods such as Gauss-Seidel and Newton-Raphson, the implementation of the HE guarantees to find the operational solution when it to be existed. Using the HE and graph [21] methods for solving the large-scale energy flow problem of a MEC in this study is a novel strategy. As shown in the next sections, the proposed decomposed strategy is faster than iterative methods such as Newton-Raphson and Gauss-Seidel which solve the PFMEC by the big Jacobian matrix for the total of the system or solve the electrical and heat sub-networks by a non-constant Jacobian matrix. In other words, due to the proposed energy flow decomposes the PFMEC problem and eliminates any non-constant Jacobian matrix in the electrical and the heat sub-networks, the iteration procedure and the time computational of the PFMEC problem have minimized. Moreover, due to that the proposed strategy utilizes the HE method which does not need the initial guesses, is more reliable than the previous methods. Finally, the taxonomy of the proposed decomposed energy flow strategy equipped with the HE and graph methods and the previous literature with details is demonstrated in Table I.

The main contributions of this paper can be summarized as:

(i) Presenting a new decomposing strategy for PF of a MEC system consisting of electrical, gas, and heating sub-networks regarding interdependent equipment with details.

(ii) Using non-iterative holomorphic embedding and less-computational graph methods in the field of energy flow of a MEC system for the power flow analysis of the electrical and heating networks.

(iii) Eliminating the time-consuming iterative procedure and non-constant Jacobian matrix in the analysis of the electrical and heat sub-networks.

(iv) Successfully validating the efficiency and the capability of the proposed strategy for the complex large-scale multi-carrier systems with the numerical simulations.

II. Multi-Energy Carrier System Model

In this section, the general model for a steady state multi-energy carrier system including electrical, gas, and heating sub-networks with respect to the energy hub is presented. The general structure for the energy hub in a MEC system is presented in Fig.1.

The energy flow shown with the solid line is related to the energy conversion equipment. However, the one with the dashed line is the energy flow received by the network and delivered to load demand without energy conversion equipment. For the analysis of any network, the related equations for the corresponding network must be solved by the proposed method. It is noted that Eqs. (1)-(2) are for the electrical network, Eqs. (3)-(12) are for the gas network, and Eqs. (13)-(20) are for the heating network.

A. Electrical Sub-Network

Equations governing electrical network are composed from two main parts. The active and reactive power flow balances for the ith bus can be expressed by:

$$P_i^{gen} + P_i^{CHP} = P_i^{dem} + P_i^{Pump} + P_i^{comp} + Re\left(V_i \sum_{j=1}^{N_E} Y_{ij}^* V_j^*\right) \quad (1)$$

$$Q_i^{gen} + Q_i^{CHP} + Q_i^{SH} = Q_i^{dem} + im(V_i \sum_{k=1}^{N_E} Y_{ij}^* V_j^*) \quad (2)$$

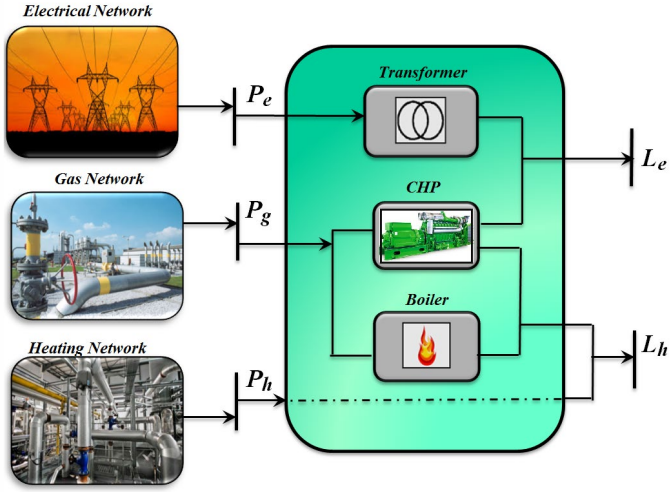

Fig. 1. The general structure for the energy hub in an MEC system

where, $\left(V_i \sum_{j=1}^{N_E} Y_{ij}^* V_j^*\right)$ represents the power that is transmitted through the line between i-th to j-th buses. In this formulation, V_i and V_j are voltage magnitudes of bus i-th and j-th while Y_{ij} is the admittance of the related transmission line. Also, N_E is the number of electrical buses.

B. Natural Gas Sub-Network

The gas network includes sources, pipelines, compressors and gas loads. The gas balance at each node and the gas flow in a pipeline can be expressed as [12]:

$$f_g^{Source} = f_g^{dem} + f^{GG} + f_{gk}^{comp} + f_G^{chp} + f_G^{boil} + \sum_{k=1}^{N_G} f_{gk} \quad (3)$$

$$f_{gk} = sign(f_{gk}) C_{gk} \left(|\pi_g^2 - \pi_k^2 - H_p^{ik}|\right)^{0.5} \quad (4)$$

$$H_p^{gk} = \frac{0.0375 g (H_g - H_k) \left(\pi_a^{gk}\right)^2}{Z_a T_a^{gk}} \quad (5)$$

$$\pi_a^{gk} = \frac{2}{3}\left[(\pi_g + \pi_k) - \left(\frac{\pi_g \pi_k}{\pi_g + \pi_k}\right)\right] \quad (6)$$

$$C_{gk} = \frac{1.14\times10^{-3} T_0 \left(D_{gk}^{GL}\right)^{2.5} E_p}{\left(L^{gk} Y_G Z_a T_a \chi_{gk}^{GL}\right)^{0.5}} \quad (7)$$

χ_{gk}^{GL} is the friction factor of the gas pipeline and is computed by the Colebrook equation as follows [22]:

$$\frac{1}{\sqrt{\chi_{gk}^{GL}}} = -2 \log\left(\frac{\varepsilon_G}{3.71 D_{gk}^{GL}} + \frac{2.51}{R_{gk}^{GL}} \frac{1}{\sqrt{\chi_{gk}^{GL}}}\right) \quad (8)$$

The flow is unrestricted in sign. In other words, if gas flow goes from node g to node k, f_{gk} comes positive and vice versa. Therefore, $sign(f_{gk})$ is a sign function of gas flow. Hence, if $f_{gk} > 0$ then the $sign(f_{gk})$ is +1 and -1 otherwise.

In the gas network, compressors are used to compensate the pressure drop at the endpoint of the pipelines. If the

compressor is driven by a gas turbine called turbo-compressor and the corresponding power consumption can be regarded as additional power flowing into the pipeline section. However, for a motor-compressor the electrical energy is provided from the electrical sub-network. The consumed horsepower by a compressor is calculated as follows [23]:

$$E_{gk}^{comp} = \frac{151.4653}{\eta_{gk}^{comp}} \frac{\pi_0}{T_0} \frac{\lambda_G}{\lambda_G - 1} z_a T_G f_{gk} \left(\left(H_{gk}^{comp} \right)^{\frac{\lambda_G - 1}{\lambda_G}} - 1 \right) \quad (9)$$

$$H_{gk}^{comp} = \frac{\pi_{k,out}^{comp}}{\pi_{g,in}^{comp}} \quad (10)$$

Hence, the electrical energy consumed provided by electrical sub-network for compressor is calculated as follows:

$$P_{E,g}^{comp} = \left(\frac{745.7 \times 10^{-6}}{3600} \right) E_{gk}^{comp} \quad (11)$$

while the amount of gas consumed provided by gas sub-network for a gas-fired turbine is computed as follows:

$$f_{gk}^{comp} = \alpha_{gk}^{comp} + \beta_{gk}^{comp} E_{gk}^{comp} + \gamma_{gk}^{comp} (E_{gk}^{comp})^2 \quad (12)$$

The parameters α_{gk}^{comp}, β_{gk}^{comp} and γ_{gk}^{comp} are consumption coefficients of the compressors.

C. Heating Sub-Network

The heating equipment using fuel like natural gas and generates heat. Heat is transferred to the heat loads via a heat transfer network. The heat power flow rate at each branch (Φ_{hb}) and the temperature at each node are as follows [21]:

$$\Phi_{hb} = \dot{m}_{hb} c_p (T_{start,h} - T_{end,b}) \quad (13)$$

$$T_{end} = (T_{start,h}, -T_g) \exp\left(\frac{L.U}{\dot{m}_{hb} c_p}\right) + T_g \quad (14)$$

where L is the pipeline length. At a node with more than one branch or supplying source, the temperature is calculated as the mixture temperature of the incoming flows as follows [17]:

$$(\sum \dot{m}_{out}) T_{out} = \sum (\dot{m}_{in} T_{in}) \quad (15)$$

Hence, in order to heat flow balance between loads and generation and lines the following equation must be satisfied:

$$\Phi_h^{Boiler} + \Phi_h^{CHP} = \Phi_h^{dem} + \sum_{b=1}^{N_H} \Phi_{hb} \quad (16)$$

In a heating network, there are circulation pumps to create the required pressure difference between the supply and return pipelines. The equation that calculates the electric power consumption by the electrical pump is found in [19].

D. Interdependencies among Sub-Networks

Electrical generators that consume natural gas relate the electrical and gas networks. The relationship between the input and output power of a gas consumed generator can be computed with dividing cost power curve by the Gross Heating Value (GHV). Accordingly, the amount of consumed fuel by the generator can be calculated by:

$$f^{GG} = \frac{1}{GHV} \left(a^{gen} \left(P_E^{gen} \right)^2 + b^{gen} P_E^{gen} + c^{gen} + \left| d^{gen} \sin \left(e^{gen} \left(P_E^{gen,min} - P_E^{gen} \right) \right) \right| \right) \quad (17)$$

The second term of Eq. (17) shows the valve-point effect [25]. In the CHPs, both heat and electrical output powers depend on each other. Generally, it is assumed that the heat power is known and fix. Note that the complete formulation and coefficients for calculating the generated electrical power of the CHPs are fully described in [26]. With having the electrical power of CHPs, the amount of natural gas consumed by CHPs can be computed using the following equation [26]:

$$f_G^{chp} = \frac{3.412}{GHV} \left(\frac{P_E^{chp} + \Phi_H^{chp}}{\eta_t^{chp}} \right) \quad (18)$$

where η_t^{chp} is the efficiency of the CHP and the factor 3.412 used to convert watt to BTU/h.

Boilers produce heat power by consuming natural gas. Similar to the CHPs, the amount of gas consumed by boilers in the heating network can be found in [19].

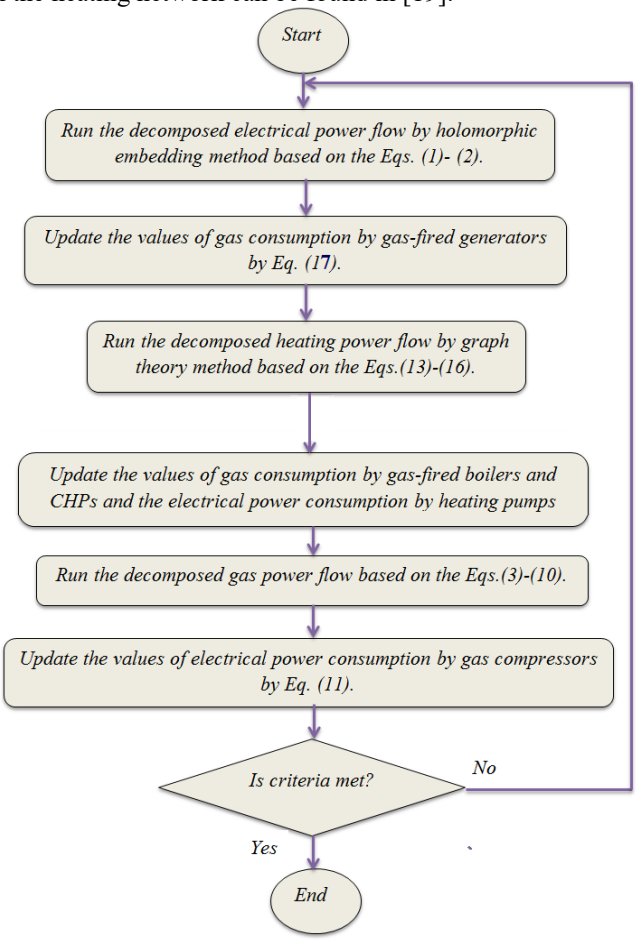

Fig. 2. Procedure for decomposing analysis of energy flow in a multi-energy carrier system

III. Proposed Decomposed Power Flow Strategy

A. Decomposing Power Flow Analysis of MEC systems

The proposed decomposing strategy determines the power flows of a MEC system consists of the heating, electrical and gas sub-networks. In this regard, the PFMEC problem is decomposed into power flow of each sub-network separately regarding the power flow of interdependent equipment among them. Due to the decomposing of PFMEC problem, the proposed strategy has more flexibility in the solution procedure of each sub-network. Moreover, the proposed decomposing strategy has more speed due to avoid making a big simultaneous Jacobin matrix for solving the PFMEC problem. Accordingly, in the decomposing analysis, we can separately utilize fast power flow methods for each sub-network. Hence, we utilize HE method which is a non-iterative and accurate electrical PF analysis method.

Moreover, the less-computational graph theory method is used to analyze the heating sub-network. The gas sub-network is solved by the Newton-Raphson technique.

For decomposing the PFMEC problem, the flow amount of interdependent equipment is initially assumed to be zeros. Then, by separately analyzing the power flow of each sub-network, the power flows of each sub-network have been determined. Afterward, by the pipeline flows of each sub-network, the power flow amounts of interdependent equipment including the gas or the electrical demand of the compressors and the electrical demand of heat pumps are approximately specified. Moreover, the approximately amount of gas consumed by slack generator if it is gas-fired is determined. After initial step these values are updated in the few next steps until all sub-networks power balances are accurately satisfied. The whole procedure for the proposed decomposed power flow of the MEC system is shown in Fig. 2. As shown in Fig.2, the solved energy flow of the first sub-network is the electrical sub-network and then heat and gas sub-networks. Then, values of interdependent equipment are updated. Since the energy flow of each sub-network is sequentially solved and dose not solve simultaneously, the different time scales of the solving energy flow of each sub-network are not significantly matter. If there are these different time scales, they do not bring a challengeable problem into energy flow solving of a multi-carrier energy.

B. Holomorphic Embedding Power Flow

The HE power flow strategy is a novel non-iterative method to solve the steady state equations of AC electrical power flow. The HE power flow method is based on a complex-valued embedding technique specifically devised to exert the specific algebraic nonlinearities of the AC power flow problem. Unlike the iterative methods such as Gauss-Seidel and Newton-Raphson, the implementation of HE guarantees to find the operational solution when there is a solution. In addition, it finds only the operational power flow solution. Holomorphic about a point is a neighborhood around that point. Hence, functions with complex variables are expressed by holomorphic functions.

On the other hand, holomorphic functions can be uniquely represented utilizing a convergent Taylor series in the neighborhood of that point. One of the complex non-holomorphic functions in the power system analyzing is the power flow problem. Hence, holomorphic embedding functions can be employed in the power flow analyzing. Since the holomorphic functions are analytic, we can use the applicable techniques to analyze the non-holomorphic electrical power flow equations. Hence, for analyzing the power flow, the formulation of the power flow should be initially become holomorphic. Then, a set of linear equations is attained that should be solved for all buses. The following equations explain the HE solution procedure for power flow analysis of all electrical nodes [20], [28].

As formerly expressed in Section II, complex electrical power can be calculated by:

$$\sum_{j=0}^{N_E} Y_{ij} V_j = \frac{S_i^*}{V_i}, \quad i \in m \tag{19}$$

One way to embed the above equation into the holomorphic is the utilizing separate series and shunt element in the admittance matrix and also utilizing an embedding variable S:

$$\sum_{j=1}^{N_E} Y_{ij\,,series}\, V_j(s) = \frac{sS_i^*}{V_i^*(s^*)} - sY_{i\,shunt} V_i(s)\,,\ i \in m \tag{20}$$

where S is the complex power, $Y_{ik\,,series}$ relates to the branch series and $Y_{i\,shunt}$ relates to the shunt element in the line data. Hence, can be expressed with:

$$Y_{ij\,,\text{series}} = \begin{cases} Y_{ii} - Y_{i\,shunt} & i = j \\ Y_{ij} & i \neq j \end{cases} \tag{21}$$

$V(s)$ in (20) is in the holomorphic form. If $V(s)$ is represented by Maclaurin series, we can express it as follows:

$$V(s) = \sum_{n=0}^{\infty} V[n]s^n = V[0] + V[1]s + \cdots + V[n]s^n \tag{22}$$

By Substituting (22) into (20), then:

$$\sum_{j=1}^{N_E} Y_{ij\,,\text{series}} \left(V_j[0] + V_j[1]s + \cdots + V_j[n]s^n\right) = \frac{sS_i^*}{\left(V_i^*[0] + V_i^*[1]s + \cdots + V_i^*[n]s^n\right)} - sY_{i\,shunt} V_i(V_i[0] + V_i[1]s + \cdots + V_i[n]s^n) \quad , \quad i \in m \tag{23}$$

$W(s)$ expresses the inverse of the voltage function in order to achieve the voltage coefficients. $W(s)$ can be defined as:

$$W(s) = \frac{1}{V(s)} = W[0] + W[1]s + \cdots + W[n]s^n \tag{24}$$

The PQ bus model is attained using the $W(s)$ expansion as:

$$\sum_{j=0}^{N_E} Y_{ij\,,\text{series}} V_j[n] = S_i^* W_i^*[n-1] - Y_{i\,shunt} V_i[n-1] \tag{25}$$

The traditional PV buses formulation is similar to the PQ buses and is expressed as follows [28]:

$$P_i = Re\left(V_i \sum_{k=1}^{N_E} Y_{ik}^* V_k^*\right),\ i \in p \tag{26}$$

$$|V_i| = V_i^{sp} \quad , \quad i \in p \tag{27}$$

where P_i determines the power generation and V_i^{sp} is the voltage magnitude at bus i. This equation can be represented in the holomorphic form as follows:

$$\sum_{j=1}^{N_E} Y_{ij\,,series}\, V_j(s) = \frac{sP_i - jQ_i(s)}{V_i^*(s^*)} - sY_{i\,shunt} V_i(s)\,,\ i \in pp \tag{28}$$

where pp defines the set of PV buses. Following equation illustrates the voltage magnitude:

$$V_i(s) * V_i^*(s^*) = 1 + s\left(\left|V_i^{sp}\right|^2 - 1\right) \quad , \quad i \in p \tag{29}$$

Moreover, the suitable holomorphic function for the voltage magnitude of the slack bus is in the following:

$$V_i(s) = 1 + \left(V_i^{sp} - 1\right)s \quad , \quad i \in slack \tag{30}$$

For more explanations about the holomorphic embedding method, please see [28].

C. Graph-Based Heat Flow

In this paper, hydraulic and thermal equations of heating networks are solved by the less-computational graph theory method [20]. The advantage of the graph theory is that the elements of utilizing matrix in this method depend on the topology of the system. Hence, unlike Jacobian matrix in the NR method, the matrix elements of the graph based method are constant and do not vary in the PF procedure. Accordingly, we only need to calculate the inverse of the incidence matrix once and save it for the overall PF procedure. A graph is commonly defined as a combination of a set of nodes, branches, and relations among them. A heating sub-network of a MEC system can be treated as a graph. In this regard, the pipes, the heat sources and the loads are represented as branches. Hence, the incidence matrix is created with N nodes and M flows (branches). The incidence matrix (A) with N×M dimensions includes the element ($a_{k,j}$) as follows [9]:

$$\begin{Bmatrix} a_{k,j} = -1 \; If \; pipe \; j \; starts \; at \; node \; k \\ a_{k,j} = 1 \; If \; pipe \; j \; ends \; at \; node \; k \\ a_{k,j} = 1 \; If \; source \; j \; ends \; at \; node \; k \\ a_{k,j} = -1 \; If \; load \; j \; starts \; at \; node \; k \\ a_{k,j} = 0 \qquad\qquad Otherwise \end{Bmatrix} \quad (31)$$

The injected or discharged mass flow rates from sources and loads are calculated as follows [9]:

$$Q_{source\ or\ load} = \dot{m}_q c_q (T_{s,source\ or\ load} - T_{r,source\ or\ load}) \quad (32)$$

The A matrix is used to calculate the heat flow of pipes by:

$$A\dot{m} = \dot{m}_q \quad (33)$$

where $\dot{m}$ is the mass flow rate in the pipes and $\dot{m}_q$ is injected or discharged mass flow rate from sources and loads. Then, (33), (13) and (14) are utilized in order to calculate the heat flow of the pipes. Moreover, flow rates in the return heat pipes are calculated in the same manner with the supply heat pipes.

It is noted that the graph method has an ability to solve the network with hydraulic loops. In the network consisting of hydraulic loops, it is essential to solve the pressure drop equation. Hence, the mass flow correction procedure is utilized in the graph method to calculate the accurate mass flow rates in the network considering pressure drops. Please see [21] for more information and a numerical example.

D. Initialization of the energy flow methods

In order to cope with the initialization points of the proposed decomposing strategy, the flow amount of interdependent equipment is initially assumed to be zero. Hence, as mentioned before, the amount of the gas or electrical demands by compressors and electrical demand by heat pumps and amount of gas consumed by the slack generator is assumed to be zero in the initial step. However, after initial step, these values are updated in the few next steps until all interdependent flows are accurately satisfied. Afterwards, for solving the decomposed electrical sub-network by the holomorphic embedding method, this method does not need any initial guess. However, for solving energy flow of the heating network, the initial points are needed for all returns and supply nodes of the heating network. These points can be initialized with equality to the value of the slack node in the heating network.

The initialization of the nodal pressures in the gas network is cumbersome. This problem is due to the fact that the gas flow through the pipelines of the gas network is a function of the difference of pressures at the pipeline's ends. Hence, if a flat level initialization is adopted for two ends of the pipeline, the Jacobian matrix of the gas network will become an ill-conditioned matrix. To cope with this issue, as expressed in [12] and [19], the initial values for the nodal pressures at the pipeline's ends are selected with a 5-10% pressures difference between the receiving and sending nodes. This technique is taken into account with the specified pressure at the slack node as a reference value. If the Newton technique is utilized for energy flow of the electrical network, it is better to initialize the values of all voltage magnitudes of non-PV buses at 1 per-unit and voltage angles of all nodes are initially selected to be zero degree. The initialization for two other networks is similar to the initialization of the two remained networks in the decomposing method.

IV. Case Studies

In order to investigate and demonstrate the efficiency and capability of the proposed decomposing strategy, the proposed strategy is tested on two MEC systems. These cases consist of electrical, heat and gas sub-networks. The simulations have been performed on MATLAB utilizing a Core i7, 2.7-GHz personal computer with 4 GB of RAM. For all cases, the part-load characteristics for boilers and CHPs are regarded.

A. Case 1

First MEC system consists of standard 14-bus IEEE test system for electrical sub-network, 20-nodes gas network and 14-nodes heating network. In this case, the electrical network consists of two generators and 20 branches. In addition, the gas network composes of 6 sources and 24 pipelines [29].

TABLE II: Data of the Sub-Networks

Electrical Network	Natural Gas Network	Heating Network
a^{chp}=0.463	GHV	$c_p = 4182(KJ/KgK)$
$b^{chp} = -0.0491$	$= 40.611\ (MBTU/m^3)$	$U = 0.2(W/mK)$
$c^{chp} = 4.49$	$\eta^{GC} = 0.8$	$\rho_W = 960$ (Kg/m3)
d_1^{chp}=0.8	$\alpha_{gk}^{comp} = \gamma_{gk}^{comp} = 0$	$g = 9.81\ (Kg.m/S^2)$
d_2^{chp}=0.6	$\beta_{gk}^{comp} = 0.0025$	$H_p = 100\ m$
e_1^{chp}=0.0736	$\varepsilon_G = 0.05\ mm$	$\eta_{HP} = 0.65$
e_2^{chp}=0.0845	$Z_a = 0.8$	$T_g = 10\ C^\circ$
$a^{GC} = 0.01(\$/MW^2)$	$\gamma_G = 0.6106$	$a^{boil} = 0.01686$
$b^{GC} = 4.0(\$/MW)$	$\lambda_G = 1.309$	b^{boil}=0.8218646
$c^{GC} = 150$ \$	$T_0 = 273.15\ K$	$\Phi_H^{boil,max}$=5 MW
$d^{GC} = 15$	$T_G = 281.15\ K$	$\eta_t^{chp} = 0.88$
$e^{GC} = 0.5$	$\pi_0 = 1.01325\ bar$	

TABLE III: Configuration of Sub-Networks for Case 1

Unit	Electric bus	Gas node	Heat node
Slack Generator	1	12	---
Generator	2	19	---
Moto-Compressor	4	9	---
Moto-Compressor	5	18	---
Slack boiler and pump	12	3	1
CHP, boiler and pump	6	15	4
CHP, boiler and pump	13	7	9
CHP, boiler and pump	14	6	10
CHP, boiler and pump	8	10	13

TABLE IV: Voltage Results Comparison in 14-Bus IEEE Case

Power Flow Method	Holomorphic Embedding		Newton-Raphson	
Node (i)	d_|V|(%)	d_θ (%)	|V|(p.u.)	θ (°)
1	0	0	1.0600	0.0000
2	0	0	1.0450	-4.9874
3	0	0	1.0100	-12.7424
4	0	0	1.0142	-10.2564
5	0	0	1.0172	-8.7646
6	0	0	1.0700	-14.4177
7	0	0	1.0503	-13.2519
8	0	0	1.0900	-13.2519
9	0	0	1.0337	-14.8323
10	0	0	1.0326	-15.0412
11	0	0	1.0475	-14.8478
12	0	0	1.0535	-15.2684
13	0	0	1.0471	-15.3081
14	0	0	1.0213	-16.0647
Computational Time (s)	0.024		0.066	

The heating network contains 13 pipelines and 9 heat sources which can be boilers or CHPs [30]. The generators in the electrical network are assumed to be gas-fired. The coefficients for the sub-networks and configuration between the units of sub-networks are given in Tables II and III, respectively. More detail about CHP and boiler units can be seen in [30].

In order to show the effectiveness of the HE method to solve PF of the electrical sub-network, the results of this method on solving 14-bus IEEE case are compared by the conventional NR method in terms of the accuracy and the time consumption in Table IV. It is clear from this table that the HE is accurate with less computational time than the NR. Since the proposed HE method does not use any Jacobian matrix, the computation speed of electrical power flow is more than the traditional iterative methods. Hence, the convergence rate of the PFMEC is increased and the solving time is decreased.

TABLE V: RESULTS COMPARISON OF VARIOUS METHODS ON CASE 1

PFMEC METHOD	Proposed DHG-PFMEC	DNR-PFMEC	NR-PFMEC
Computational Time (s)	0.089	0.114	0.122

TABLE VI: ELECTRICAL VOLTAGE RESULTS COMPARISON IN CASE 1

PFMEC Method	Proposed DHG-PFMEC		DNR-PFMEC		NR-PFMEC	
Node	d_|V|(%)	d_θ (%)	d_|V|(%)	d_θ (%)	|V|(p.u.)	θ (°)
1	0	0	0	0	1.060	0.00
2	0	0	0	0	1.040	-3.13
3	0	0.012	0.515	0.289	0.969	-10.37
4	-0.03	0	0.302	0.258	0.992	-7.74
5	0	0	0.299	0.311	1.000	-6.43
6	0	0	0	0.097	1.030	-10.24
7	-0.04	0	0.1	0.212	0.999	-9.39
8	0	0.045	0	0.358	1.000	-8.37
9	-0.04	0.007	0.1	0.183	0.991	-10.91
10	-0. 05	0	0.101	0.18	0.990	-11.10
11	-0.019	0	0	0.092	1.006	-10.80
12	0	0.009	0	0.091	1.019	-10.94
13	0	0	0	0	1.020	-10.90
14	0	0	0	0	1.000	-11.33

To investigate the efficiency of the proposed Decomposing PFMEC strategy with Holomorphic and Graph methods (denoted as DHG-PFMEC) in terms of the accuracy and the time consumption, a comparison between results of it, Newton-Raphson-PFMEC (NR-PFMEC) method and Decomposed Newton-Raphson-PFMEC (DNR-PFMEC) method is presented. The DNR-PFMEC method is a decomposed procedure like the proposed DHG-PFMEC method while it employs NR method to solve the electrical sub-network instead of the HE method. Moreover, the NR-PFMEC is a coupling method for PFMEC solving utilizing a simultaneous Jacobian matrix for three sub-networks [19].

The energy flow problem of mentioned test system has 81 state variables. The solutions were obtained with a mismatch tolerance of 10^{-5} in the values of interdependent equipment.

Table V shows the computational time results obtained by the DHG-PFMEC strategy, DNR-PFMEC and NR-PFMEC methods. As seen from Table V, all PFMEC methods can solve the power flow problem of the integrated system. The computation time of the proposed DHG-PFMEC strategy, DNR-PFMEC and NR-PFMEC are 0.089, 0.114 and 0.122 seconds, respectively. It indicates that DNR-PFMEC is faster 28% and 22% more than DNR-PFMEC and NR-PFMEC, respectively. It is notable that the proposed DHG-PFMEC strategy only needs 3 steps to converge the interdependent values of MEC system including electrical power consumed by the heating pumps and compressors as well as gas consumed by generators. The result comparisons among three mentioned methods including bus voltages, gas pressures and supply and return temperatures are summarized in Tables VI-VIII. In these tables, the results of DHG-PFMEC strategy and DNR-PFMEC method are compared with the results of NR-PFMEC method in terms of the accuracy and have been brought by percentage of the deviation from NR-PFMEC method by d_|V|, d_θ, d_P_i and d_T_i^S. It can be realized from these tables that the results of DHG-PFMEC strategy is very close to the results of NR-PFMEC method in terms of the accuracy.

TABLE VII: GAS PRESSURE RESULTS COMPARISON IN CASE 1

PFMEC Method	DHG	DNR	NR	PFMEC Method	DHG	DNR	NR
Node (g)	d_π_g (%)	d_π_g (%)	π_g (bar)	Node (g)	d_π_g (%)	d_π_g (%)	π_g (bar)
1	0	0	56.00	11	0	0	55.65
2	0	0	55.96	12	0	0	53.84
3	0	0	55.81	13	0	0	52.73
4	0	0	53.99	14	0	0	52.56
5	0	0	52.81	15	0	0	51.21
6	0	0	52.06	16	0	0	49.54
7	0	0	52.17	17	0	0	54.58
8	0	0	49.43	18	0	0	45.10
9	0	0	48.89	19	0	0	31.84
10	0	0	56.83	20	0	0	29.69

TABLE VIII: HEATING TEMPERATURES RESULTS COMPARISON IN CASE 1

PFMEC Method	Proposed DHG-PFMEC		DNR-PFMEC		NR-PFMEC	
Node (h)	d_T_h^S(%)	d_T_h^r(%)	d_T_h^S(%)	d_T_h^r(%	$T_h^S(C)$	$T_h^r(C)$
1	0	0	0	0	120.00	48.01
2	0	-0.02	0	-0.02	117.69	48.83
3	-0.008	0	-0.008	0	116.98	50.00
4	0.016	0	0.016	0	118.38	48.95
5	0	0.02	0	0.02	117.14	49.40
6	0	0.02	0	0.02	116.58	49.47
7	-0.008	0	-0.008	0	116.12	50.00
8	0	0	0	0	115.87	50.00
9	0.008	0	0.008	0	122.74	46.92
10	0	-0.02	0	-0.02	119.38	48.46
11	0	0	0	0	117.65	49.07
12	0	0	0	0	116.93	50.00
13	0.008	-0.02	0.008	-0.02	117.43	49.66
14	0	0	0	0	116.49	50.00

B. Case 2

In order to test the validity of the proposed DHG-PFMEC strategy on solving large-scale PFMEC problems, the proposed strategy is tested on a large-scale MEC system. Hence, the large-scale MEC system including the modified 118-bus IEEE system [31], the 48-bus natural gas system [32] - [33] and 14-nodes heating system [30] is utilized. The MEC system has 54 thermal units including 12 natural gas-fired units, 4 CHP units, 5 boilers, 2 heat pumps, 9 natural gas sources and 8 compressors (5 motor compressors and 3 turbo-

compressors). Each electrical, gas and heating network consists of 186, 43 and 13 branches, respectively. The configuration between units and the energy hubs for this case are presented in Table IX.

TABLE IX: CONFIGURATION OF SUB-NETWORKS FOR CASE 2

Unit	Electric	Gas	Heat
Generator	10	30	---
Generator	12	36	---
Generator	25	29	---
Generator	26	45	---
Moto-Compressor	10	12-13	---
Moto-Compressor	65	20-21	---
Moto-Compressor	65	21-22	---
Moto-Compressor	65	20-48	---
Moto-Compressor	65	48-25	---
Slack boiler and pump	82	20	1
CHP, boiler and pump	60	3	4
CHP, boiler and pump	45	5	9
CHP, boiler and pump	11	7	10
CHP, boiler and pump	66	15	13

TABLE X: VOLTAGE RESULTS COMPARISON IN 118-BUS IEEE CASE

Power Flow Method	Holomorphic Embedding Method		Newton-Raphson Method	
Node (i)	d_|V|(%)	d_θ	|V|(p.u.)	θ (∘)
8	0	-0.047	1.015	21.03
36	0	0.09	0.980	11.08
66	0	0	1.050	27.55
87	0	0.031	1.015	31.44
104	0	0	0.971	21.74
116	0	0	1.005	27.17
Computational Time (s)	0.175		0.275	

TABLE XI: COMPARISON RESULTS OF VARIOUS METHODS ON CASE 2

PFMEC METHOD	Proposed DHG-PFMEC	DNR-PFMEC	NR-PFMEC
Computational Time (s)	0.261	0.624	Did not converge

TABLE XII: COMPARISON RESULTS OF VARIOUS METHODS ON CASE 2

Sub-network	PFMEC Method	Proposed DHG-PFMEC		DNR-PFMEC	
Electrical	Node (i)	d_|V|(%)	d_θ (%)	|V|(p.u.)	θ (∘)
	45	-0.074	0	0.992	16.8
	60	-0.085	0	0.998	24.0
	66	-0.053	0.057	1.054	28.1
	82	0.061	0.042	0.984	27.8
Heating	Node (h)	d_T_h^S(%)	d_T_h^r(%)	$T_h^s(C)$	$T_h^r(C)$
	1	0	0	120.00	48.0
	6	0	0.02	116.57	49.4
	11	0	0	117.65	49.0
	13	0	-0.02	117.43	49.6
Natural Gas	Node (g)	d_π_g(%bar)		π_g(bar)	
	12	0		55.34	
	20	0		49.95	
	26	0		67.17	
	29	0		58.06	

To test the applicability of holomorphic embedding method in large-scale electrical sub-networks, the PF results of the HE method and the conventional NR method for the 118-bus IEEE system have been compared in Table X. It is evident that the HE method can accurately solve the large-scale electrical power flow with less computational time than the NR method.

Since MEC system in case 2 is large-scale, the feasible solution for PFMEC problem of this system is computational and troublous. Fortunately, the high computational efficiency and feasible applicability of the proposed strategy could greatly diminish this problem. Table XI presents the calculation time of various PFMEC methods. As shown from this table, no feasible solution can be obtained by NR-PFMEC method while the proposed decomposing DHG-PFMEC and DNR-OPF methods could reach to a feasible solution. It is noteworthy to say that the Jacobian matrix size that the NR-PFMEC method needs to inverse for this case is 257×257. Accordingly, the NR-PFMEC method with big variable Jacobian matrix could not converge for this large-scale system. However, the proposed DHG-PFMEC strategy accurately solves the power flow problem within 0.261 seconds which is faster 58% more than the DNR-PFMEC method. It is obvious that proposed DHG- PFMEC strategy is faster than DNR-PFMEC method to solve the large-scale power flow of the MEC system. Due to the proposed strategy does not utilize inverse of a Jacobian with variable elements in each iteration of electrical and heating sub-networks like NR-PFMEC and DNR-PFMEC methods, the computational time of the proposed strategy is less than the other methods. Also, it is capable to reach a feasible and reliable solution in the electrical sub-network by Holomorphic embedding due to it is not initial guess depending. The proposed DHG-PFMEC strategy converged only in six steps for the value of interdependent equipment. The comparison PFMEC results of DHG-PFMEC and DNR-PFMEC methods are displayed in Table XII. The accurate results of the proposed PFMEC show that this method effectively solves the large-scale problem.

In order to investigate the performance of the proposed decomposing strategy on solving a MEC system with high interdependency between the three networks, Case 2 has been extended. In this regard, the existing numbers of CHPs and boilers and electrical pumps have been become double. Moreover, the generation heat values of CHPs and boilers have been become triple of the previous values. Thus, four surplus CHPs, boilers and heating pump are placed in the MEC system of Case 2. The configuration of surplus equipment is shown in Table XIII.

TABLE XIII: CONFIGURATION OF SUB-NETWORKS FOR EXTENDED CASE 2

Unit	Electrical	Gas	Heat	Heat Generation (MW)
CHP	84	9	3	60
CHP	86	13	5	60
CHP	95	14	6	75
CHP	108	11	7	75
Boiler	---	9	3	15
Boiler	---	13	5	9
Boiler	---	14	6	6
Boiler	---	11	7	15
Electrical Heat Pump	84	---	3	---
Electrical Heat Pump	86	---	5	---
Electrical Heat Pump	95	---	6	---
Electrical	108	---	7	---

Heat Pump

TABLE XIV: COMPARISON RESULTS OF DHG-PFMEC METHOD ON EXTENDED CASE 2 WITH HIGH INTERDEPENDENCIES

Sub-network	PFMEC Method	Proposed DHG-PFMEC	
Electrical	Node (i)	|V|(p.u.)	θ (∘)
	45	0.987	20.147
	60	0.993	26.774
	66	1.050	30.404
	82	0.989	34.980
Heating	Node (h)	$T_h^s(C)$	$T_h^r(C)$
	1	120.00	51.002
	6	119.658	49.452
	11	121.051	49.960
	13	120.397	49.631
Natural Gas	Node (g)	π_g (bar)	
	12	54.008	
	20	48.126	
	26	63.130	
	29	53.173	
Computational Time (s)		0.307	

TABLE XV: VOLTAGE RESULTS COMPARISON IN 6468TRE-CASE

Power Flow Method	Holomorphic Embedding Method		Newton-Raphson Method	
Node (i)	d_|V|(%)	d_θ (%)	|V|(p.u.)	θ (∘)
57	0	-0.021	1.059	-18.74
473	0	0	1.04	-20.52
762	0	0.05	1.034	-12.89
2506	0	0	1.009	-20.42
2851	0	0.095	1.04	-13.87
4051	0	0.046	0.88	-15.28
Computational Time (s)	1.32		1.51	

TABLE XVI: COMPARISON RESULTS OF VARIOUS METHODS ON CASE 3

PFMEC METHOD	Proposed DHG-PFMEC	DNR-PFMEC	NR-PFMEC
Computational Time (s)	2.13	2.56	not converged

The energy flow results of this extended MEC by the proposed decomposing strategy are presented in Table XIV. It can be seen from this table that the proposed DHG-PFMEC method can solve the extended MEC with high interdependency by 0.307 second which is 0.046 second more than original Case 2. It is notable that the proposed DHG-PFMEC strategy converged only in seven steps for the high interdependent equipment.

C. Case 3

In order to demonstrate conclusively the superiority of the proposed DHG-PFMEC method with respect to the DNR-PFMEC and NR-PFMEC methods, we decided to simulate a large-scale case with more complexities. Hence, we tested our proposed DHG-PFMEC method on a MEC system including 6468rte-case electrical network [33], previous 48-bus gas network and previous 20-nodes heating network with added two hydraulic loops [33] which increase the complexity of the problem. In addition, the results are compared with the results of the DNR-PFMEC and the NR-PFMEC methods. The MEC system has 1295 generators and 9000 electrical branches.

The PF results of HE method and conventional NR method for the electrical 6468rte-bus network are compared in Table XV. It is notable that the applicability of the holomorphic embedding method in large-scale electrical sub-networks is shown by the results of Table XV. In this case, the HE method can accurately solve the large-scale electrical power flow with less computational time than the NR method.

The proposed energy flow method in case 3 must specify 11715 variables including 28 values for the heating network, 47 values for the gas network and 11640 values for the electrical network, respectively. The computational times of various methods on solving case 3 are presented in Table XVI. It is noteworthy to say that NR-PFMEC method cannot converge in this case like case 2. The proposed DHG-PFMEC strategy accurately solves the energy flow of MEC system in case 3 within 2.13 seconds which is 17% faster than the DNR-PFMEC method.

The results of DNR-PFMEC and the deviation values of PFMEC results from DNR-PFMEC are shown in Table XVII. It is notable that the decomposing strategy helps the speed and convergence rate of the proposed DHG-PFMEC in this complex case.

TABLE XVII: COMPARISON RESULTS OF VARIOUS METHODS ON CASE 3

Sub-network	PFMEC Method	Proposed DHG-PFMEC		DNR-PFMEC	
Electrical	Node (i)	d_|V|(%)	d_θ (%)	|V|(p.u.)	θ (∘)
	45	0.057	0.042	0.992	16.507
	60	0.061	-0.008	0.998	23.847
	3990	0.036	-0.021	1.026	-3.282
	6086	-0.042	0.067	1.042	15.914
Heating	Node (h)	$d\_T_h^S(\%)$	$d\_T_h^r(\%)$	$T_h^s(C)$	$T_h^r(C)$
	1	0	0	120.00	47.11
	6	0.01	0	120.54	49.62
	11	0	0.02	121.25	48.02
	13	0	0	124.95	49.73
Natural Gas	Node (g)	d_πg (%bar)		πg (bar)	
	12	0		58.64	
	20	0		48.45	
	26	0		69.23	
	29	0		61.46	

V. CONCLUSIONS

A novel decomposing energy flow strategy for a multi-energy carrier system with electrical, natural gas and heating sub-networks has been proposed in this paper. For this aim, the interdependent equipment among sub-networks such as CHPs, boilers and electrical pump are taken into account. The proposed energy flow used in this paper minimizes the iteration procedure of the energy flow and accelerates the computation by decomposing the PFMEC problem and eliminates any non-constant Jacobian matrix in the electrical and the heat sub-networks based on the novel non-iterative HE and less-computational graph-based methods. The numerical results demonstrate that the proposed decomposing strategy can solve the MEC power flow accurately with less computational time than Newton-Raphson method. The superiority and applicability of the proposed decomposing strategy are salient comparing to the coupling iterative

methods like Newton-Raphson for the simultaneous solution of the large-scale power flow of MEC systems. The results showed that for solving the large-scale MEC energy flows, it is essential to use the decomposing strategy to reach the feasible solution.

REFERENCES

[1] C. He, L. Wu, T. Liu, and M. Shahidehpour, "Robust Co-Optimization Scheduling of Electricity and Natural Gas Systems via ADMM," *IEEE Trans. Sustain. Energy*, vol. 8, no. 2, pp. 658 - 670, 2017.

[2] Z. Li, and et al., "Transmission-Constrained Unit Commitment Considering Combined Electricity and District Heating Networks," *IEEE Trans. Sustain. Energy*, vol. 7, no. 2, pp. 480 - 492, 2016.

[3] Z. Ren, K. Wang, l. Wenyuan, L. Jin, and Y. Dai, "Probabilistic Power Flow Analysis of Power Systems Incorporating Tidal Current Generation," *IEEE Trans. Sustain. Energy*, vol. PP, no. 99, pp. 1 - 9, 2017.

[4] M. Mikolajková, C. Haikarainen, H. Saxén, and F. Pettersson, "Optimization of a natural gas distribution network with potential future extensions," *Energy*, vol. 125, pp. 848–859, 2017.

[5] J. Dorfner, and T. Hamacher, "Large-Scale District Heating Network Optimization," *IEEE Trans. Smart Grid*, vol. 5, no. 4, pp. 1884-1891, 2014.

[6] R. Frik, and P. Favre-Perrod, "Proposal for a multifunctional energy bus and its interlink with generation and consumption," diploma thesis, Power Systems and High Voltage Laboratories, ETH, Zurich, Switzerland, 2004.

[7] M. Geidl, and et al., "Energy hubs for the future," *IEEE Power and Energy Magazine*, vol. 5, no. 1, pp. 24-30, 2007.

[8] M. M. Aghtaie, P. Dehghanian, M. Fotuhi-Firuzabad, and A. Abbaspour, "Multiagent Genetic Algorithm: An Online Probabilistic View on Economic Dispatch of Energy Hubs Constrained by Wind Availability," *IEEE Trans. Sustain. Energy*, vol. 5, no. 2, pp. 699 - 708, 2014.

[9] S. Bahrami, and A. Sheikhi, "From Demand Response in Smart Grid Toward Integrated Demand Response in Smart Energy Hub," *IEEE Trans. Smart Grid*, vol. 7, no. 2, pp. 650-658, 2016.

[10] A. Najafi, H. Falaghi, J. Contreras, and M. Ramezani, "A Stochastic Bilevel Model for the Energy Hub Manager Problem," *IEEE Trans. Smart Grid*, vol. PP, no. 99, pp. 1-11, 2016.

[11] A. Quelhas, E. Gil, J. D. McCalley, and S. M. Ryan, "A multiperiod generalized network flow model of the U.S. integrated energy system: Part I—Model description," *IEEE Trans. Power Syst.*, vol. 22, no. 2, pp. 829–836, May 2007.

[12] A. Martínez-Mares, and C. R. Fuerte-Esquivel, "A Unified Gas and Power Flow Analysis in Natural Gas and Electricity Coupled Networks," *IEEE Trans. Power Syst.*, vol. 27, no. 4, pp. 2156-2166, 2012.

[13] M. Geidl and G. Andersson, "Optimal power flow of multiple energy carriers," *IEEE Trans. Power Syst*., vol. 22, no.1, pp. 145-155, 2007.

[14] X. Zhang, and et al., "Reliability-Based Optimal Planning of Electricity and Natural Gas Interconnections for Multiple Energy Hubs," *IEEE Trans. Smart Grid*, vol. PP, no. 99, pp. 1-10, 2015.

[15] P. Mancarella, and G. Chicco, "Real-Time Demand Response from Energy Shifting in Distributed Multi-Generation," *IEEE Trans. Smart Grid*, vol. 4, no. 4, pp. 1928 - 1938, 2013.

[16] N. Neyestani, M. Yazdani-Damavandi, M. Shafie-khah, G. Chicco, and J.P.S. Catalão, "Stochastic Modeling of Multienergy Carriers Dependencies in Smart Local Networks with Distributed Energy Resources," *IEEE Trans. Smart Grid*, vol. 6, no. 4, pp. 1748 - 1762, 2015.

[17] Z. Li, and et al., "Combined Heat and Power Dispatch Considering Pipeline Energy Storage of District Heating Network," *IEEE Trans. Sustain. Energy*, vol. 7, no. 1, pp. 12-22, 2016.

[18] M. Moeini-Aghtaie, A. Abbaspour, M. Fotuhi-Firuzabad, and E. Hajipour, "A Decomposed Solution to Multiple-Energy Carriers Optimal Power Flow," *IEEE Trans. Power Syst.*, vol. 29, no. 2, pp. 707-716, 2014.

[19] A. Shabanpour-Haghighi, and A. R. Seifi, "An integrated steady state operation assessment of electrical, natural gas, and district heating networks" *IEEE Trans. Power Syst.*, vol. 31, no. 5, pp. 3636 - 3647, 2016.

[20] H.-D. Chiang, T. Wang, and H. Sheng, "A Novel Fast and Flexible Holomorphic Embedding Method for Power Flow Problems," *IEEE Trans. Power Syst*., vol. PP, no. 99, pp. 1-12, 2017.

[21] M. Pirouti, "Modeling and Analysis of a District Heating Network," Ph.D. thesis, Institute of Energy, Cardiff Univ., Cardiff, Wales, 2013.

[22] D. Clamond, "Efficient resolution of the Colebrook equation," *Industrial & Engineering Chemistry Research*, vol. 48, no. 7, pp. 7-23, 2008.

[23] B. Bakhouya, and D. De Wolf, "Solving gas transmission problems by taking compressors into account," Univ. littoral Opal. Coast, Dunkerque, France, 2008.

[24] X. Liu, "Combined analysis of electricity and heat networks," Ph.D. dissertation, Institute of Energy, Cardiff Univ., Cardiff, Wales, 2013.

[25] A. Shukla and S. Singh, "Pseudo-inspired CBA for ED of units with valve-point loading effects and multi-fuel options," *IET Generation, Transmission & Distribution*, vol. 11, no. 4, pp. 1039 - 1045, 2017.

[26] T. Savola and I. Keppo, "Off-design simulation and mathematical modeling of small-scale CHP plants at part loads," *Appl. Thermal Eng.*, vol. 25, no. 8, pp. 1219–1232, 2005.

[27] T. H. Durkin, "Boilers system efficiency," *ASHRAE J.*, vol. 48, no. 7, pp. 51-58, 2006.

[28] S. Rao, Y. Feng, D. J. Tylavsky, and M. Kumar Subramanian, "The Holomorphic Embedding Method Applied to the Power-Flow Problem," *IEEE Trans. Power Syst.*, vol. 31, no. 5, pp. 3816 - 3828, 2016.

[29] D. De Wolf and Y. Smeers, "The gas transmission problem solved by an extension of the simplex algorithm," Manage. Sci., vol. 46, no. 11, pp. 1454–1465, Nov. 2000.

[30] A. Shabanpour-Haghighi, and A. R. Seifi, "Simultaneous Integrated Optimal Energy Flow of Electricity, Gas, and Heat," *Energy Conversion and Management*, vol.101, pp. 579–591, June. 2015.

[31] http://motor.ece.iit.edu/data/SCUC_118

[32] S. Wu, R. Z. Ríos-Mercado, E. Boyd, and L. Scott, "Model relaxation for the fuel cost minimization of steady-state gas pipeline networks, " *Math. Comput. Model*, vol. 31, no. 23, pp. 197–220, 2000.

[33] https://figshare.com/s/ff054e801bd3459ad8ab